

# Intestinal Infection Is Associated With Impaired Lung Innate Immunity to Secondary Respiratory Infection

Shubhanshi Trivedi,<sup>1</sup> Allie H. Grossmann,<sup>3,5,6</sup> Owen Jensen,<sup>1</sup> Mark J. Cody,<sup>4</sup> Taylor A. Wahlig,<sup>1</sup> Paula Hayakawa Serpa,<sup>8,9</sup> Charles Langelier,<sup>8,9</sup> Kristi J. Warren,<sup>2</sup> Christian C. Yost,<sup>4,6</sup> and Daniel T. Leung<sup>1,7,○</sup>

<sup>1</sup>Division of Infectious Disease, Department of Internal Medicine, University of Utah, Salt Lake City, Utah, USA, <sup>2</sup>Division of Pulmonary Medicine, Department of Internal Medicine, University of Utah, Salt Lake City, Utah, USA, <sup>3</sup>Huntsman Cancer Institute, University of Utah, Salt Lake City, Utah, USA, <sup>4</sup>Division of Neonatology, Department of Pediatrics, University of Utah, Salt Lake City, Utah, USA, <sup>5</sup>Division of Anatomic Pathology, Department of Pathology, University of Utah, Salt Lake City, Utah, USA, <sup>6</sup>Molecular Medicine Program, University of Utah, Salt Lake City, Utah, USA, <sup>7</sup>Division of Microbiology and Immunology, Department of Pathology, University of Utah, Salt Lake City, Utah, USA, <sup>8</sup>Chan Zuckerberg Biohub, San Francisco, California, USA, and <sup>9</sup>Division of Infectious Diseases, Department of Medicine, University of California-San Francisco, San Francisco, California, USA

**Background.** Pneumonia and diarrhea are among the leading causes of death worldwide, and epidemiological studies have demonstrated that diarrhea is associated with an increased risk of subsequent pneumonia. Our aim was to determine the impact of intestinal infection on innate immune responses in the lung.

**Methods.** Using a mouse model of intestinal infection by *Salmonella enterica* serovar Typhimurium (*S. Typhimurium* [ST]), we investigated associations between gastrointestinal infections and lung innate immune responses to bacterial (*Klebsiella pneumoniae*) challenge.

**Results.** We found alterations in frequencies of innate immune cells in the lungs of intestinally infected mice compared with uninfected mice. On subsequent challenge with *K. pneumoniae*, we found that mice with prior intestinal infection have higher lung bacterial burden and inflammation, increased neutrophil margination, and neutrophil extracellular traps, but lower overall numbers of neutrophils, compared with mice without prior intestinal infection. Total numbers of dendritic cells, innate-like T cells, and natural killer cells were not different between mice with and without prior intestinal infection.

**Conclusions.** Together, these results suggest that intestinal infection impacts lung innate immune responses, most notably neutrophil characteristics, potentially resulting in increased susceptibility to secondary pneumonia.

**Keywords.** diarrhea; pneumonia; innate immunity; neutrophils; NETs.

Diarrhea and pneumonia are among the leading causes of death worldwide. In children alone, these diseases combine to kill ~1.4 million each year, with the majority of these deaths occurring in lower- and middle-income countries [1]. Epidemiological studies have shown that children are at an increased risk of pneumonia following a diarrheal episode [2, 3]. However, the immunological mechanisms behind an increased susceptibility to such secondary respiratory infections are not well understood.

Although the gastrointestinal and respiratory tracts have different environments and functions, there are emerging data showing crosstalk between these 2 mucosal sites in chronic inflammatory diseases such as inflammatory bowel disease (IBD) and asthma [4]. Additionally, there is emerging evidence that the intestinal microbiota plays a role in host defense against

bacterial pneumonia [5]. The gastrointestinal and respiratory tracts share the same embryonic origin and have common components of the mucosal immune system such as an epithelial barrier, submucosal lymphoid tissue, the production of IgA and defensins, and the presence of innate lymphocytes and dendritic cells [6]. Notably, several innate-like leukocytes, such as mucosal-associated invariant T (MAIT) cells, invariant natural killer T (iNKT) cells, gamma delta T ( $\gamma\delta$  T) cells, dendritic cells (DCs) and neutrophils, have the capacity to circulate between tissues and play important roles in both respiratory and intestinal tract immunity [7, 8].

*Salmonella enterica* subspecies 1 serovar Typhimurium (ST) is a principal cause of human enterocolitis. In mice, serovar Typhimurium does not normally provoke intestinal inflammation or develop diarrhea [9]; however, the streptomycin-pretreated mouse model for *Salmonella* diarrhea [10] has emerged as an excellent tool to study pathogen–host interactions in the intestinal mucosa. Without streptomycin pretreatment, oral infection with ST leads to enteropathy in only 5% of all animals, but upon treatment with a single dose of streptomycin, infected animals develop pronounced mucosal inflammation as early as 4–8 hours postinfection [10, 11]. Furthermore, the time course of the disease, the histopathology, the cytokine response patterns of the infected mucosa, and the disease-eliciting virulence factors of the pathogen are virtually identical between

Received 11 March 2021; editorial decision 3 May 2021; accepted 5 May 2021.

Correspondence: Daniel T. Leung, MD, 26 North Medical Drive, Salt Lake City, UT 84132 (daniel.leung@utah.edu).

Open Forum Infectious Diseases® 2021

© The Author(s) 2021. Published by Oxford University Press on behalf of Infectious Diseases Society of America. This is an Open Access article distributed under the terms of the Creative Commons Attribution-NonCommercial-NoDerivs licence (<http://creativecommons.org/licenses/by-nc-nd/4.0/>), which permits non-commercial reproduction and distribution of the work, in any medium, provided the original work is not altered or transformed in any way, and that the work is properly cited. For commercial re-use, please contact journals.permissions@oup.com  
DOI: 10.1093/ofid/ofab237

streptomycin-pretreated mice and bovine and primate models of the disease [12].

Overall, pretreatment of mice with streptomycin renders them susceptible to serovar Typhimurium colitis, which closely resembles the inflammatory responses observed in the human colon. Therefore, in this study, we examine the impact of intestinal infection on the immune response in the lungs of mice using this established model of intestinal infection [10]. We found that mice infected with *S. Typhimurium* have increased susceptibility to respiratory *Klebsiella pneumoniae* (*KP*) infection compared with mice without prior intestinal infection. Prior intestinal infection modulated effector cells of innate immunity in the lung, contributing to respiratory immune dysregulation and a higher *KP* bacterial burden.

## METHODS

### Mice and Inoculations

Six- to 8-week-old female C57BL/6J wild-type mice were obtained from Jackson Laboratories. All animals were maintained and experiments were performed in accordance with University of Utah and Institutional Animal Care and Use Committee guidelines (protocol 17-01011). The animals were kept at a constant temperature (25°C) with unlimited access to pellet diet and water in a room with a 12-hour light/dark cycle. All animals were monitored daily, and infected animals were scored for the signs of clinical illness severity [13]. Animals were ethically killed using CO<sub>2</sub>.

For the experiments, all mice were pretreated with streptomycin as described previously [10]. Briefly, water and food were withdrawn 4 hours before oral gavage treatment with 7.5 mg of streptomycin in 100 µL of HBSS. Afterward, animals were supplied with water and food ad libitum. At 20 hours after streptomycin treatment, water and food were withdrawn again for 4 hours before mice were gavaged with 10<sup>4</sup> CFU of *ST* (100-µL suspension in phosphate-buffered saline [PBS]) or treated with sterile PBS (control). Thereafter, drinking water and food ad libitum was offered immediately. Six days postinfection, mice were killed, and lungs removed for analysis.

For *KP* challenge experiments, 6 days post-*ST* infection, isoflurane-anesthetized mice were inoculated intranasally with high-inoculum ~10<sup>10</sup> CFU *KP* in a 50-µL volume. Inoculated mice were killed at 18 hours for bacterial load enumeration and immune assessment (details of bacterial strains and dosing justifications are available in the [Supplementary Methods](#)).

### Lung Histology

After death, mouse lungs were infused with 10% neutral buffered formalin via the trachea, fixed in formalin overnight, dehydrated in 70% ethyl alcohol, and embedded in paraffin; 4-µm sections were stained with hematoxylin and eosin and analyzed by a board-certified anatomic pathologist (A.H.G.). Samples were blinded before histopathologic analysis.

### Lung Neutrophil Extracellular Trap Assessment

Paraffin-embedded mouse lungs were cut to 8-µm thickness on a microtome. Sections were deparaffinized and rehydrated using xylene and decreasing ethanol concentration washes. Heat-induced epitope antigen retrieval of lung sections were processed in a 2100 Retriever Thermal Processor (Electron Microscopy Sciences) containing Citrate buffer pH 6.0 solution. Sections were incubated for 10 minutes with 0.1% Triton-X-100 and blocked with 10% Donkey Serum for 1 hour at room temperature (RT). Antibodies for citrullinated Histone H3 (Abcam) and myeloperoxidase (MPO; R&D Systems) were incubated at 1:100 dilution in 10% donkey serum overnight at 4°C. After washing sections with PBS, secondary rabbit and goat antibodies conjugated to Alexa Fluor 488 or Alexa Fluor 546, respectively, along with DAPI nuclear stain, were incubated on sections for 90 minutes at 4°C. Sections were washed, and coverslips were adhered with aqueous mounting medium (Dako, S3025). Images were acquired on an Olympus FV3000 Confocal Laser Scanning Microscope. FluoView software (Olympus) and ImageJ Fiji (NIH) were used for image processing and analysis. We quantified neutrophil extracellular trap (NET) formation on the images using a standardized grid system [14]. Briefly, we placed a standardized grid on randomly selected high-power field images (n = 5 field images/sample). The number of times that any NET crossed a grid line was tallied.

### Lung Mononuclear Cell Isolation

For lung digestion and preparation of single-cell suspensions, lungs were perfused using 5 mL of PBS, aseptically harvested from dead mice, and kept in RPMI with 10% fetal bovine serum (FBS). Lungs were dissociated using the mouse Lung Dissociation Kit (Miltenyi Biotec) and the gentleMACS Dissociator (Miltenyi Biotec). Cells were then passed through a 70-µm cell strainer and washed. Red blood cells were lysed with red blood cell lysis buffer. Lung mononuclear cells were then washed twice.

### Bacterial Load Quantification

*KP* bacterial load was determined by plating 10-fold serial dilutions of the lung homogenates onto MacConkey agar plates (Sigma-Aldrich). The plates were incubated at 37°C overnight before bacterial CFUs were determined by colony counts.

### Mouse Inflammation Quantification

Lungs homogenates were filtered on 70-µm cell strainers and centrifuged at 300 × g for 5 minutes. Supernatants were stored at -80°C for cytokine content analysis. Lung cytokine levels were assessed from the supernatant samples via the LEGENDplex kit (mouse inflammation panel 13-plex, BioLegend), per the manufacturer's instructions. Cytokine levels were acquired using a FACSCanto II flow cytometer (BD Biosciences), and

analyses were performed using LEGENDplex data analysis software (BioLegend).

#### Tetramer and Antibody Surface Staining of Lung Single-Cell Suspensions

From each animal, 1–2 million-cell aliquots were prepared and stained with the fixable viability dye eFluor 780 (eBioscience) for 15 minutes at RT to exclude dead cells and washed with PBS + 2% FBS and incubated with antimouse CD16/CD32 Fc Block antibody (BD) for 20 minutes at 4°C. Cells were then stained for 30 minutes with fluorescence-conjugated antibodies at either RT or 4°C (detailed in the [Supplementary Methods](#)). A total of  $10^6$  gated events per sample were collected using the BD Fortessa flow cytometer, and results were analyzed using FlowJo 10.4.2 software.

#### Statistical Analysis

GraphPad Prism 8 software was used for statistical analysis. The Mann-Whitney *U* test was used for comparison between uninfected and *ST*-infected groups and between mice with and without prior intestinal infection. Results were presented as mean  $\pm$  SD, and  $P < .05$  was considered statistically significant.

## RESULTS

### Mice With Prior *ST* Intestinal Infection Have Increased Lung Bacterial Load, Sickness Score, and Susceptibility to Respiratory *KP* Infection

To test whether prior intestinal infection increases the susceptibility to respiratory *KP* infection, we evaluated survival, body weight loss, sickness score, and bacterial burden in lungs post-*KP* challenge ([Figure 1A](#)). Compared with *ST*-infected mice, which had a survival rate of 90%–100%, and *K. pneumoniae*-infected mice, which had a survival rate of 60%–80%, mice with prior *ST* intestinal infection had a survival rate of 0%–30% at 120 hours post-*KP* infection ([Figure 1B](#)). Interestingly, although there were no statistically significant differences in body weight loss between mice with vs without *ST* infection with *KP* challenge ([Supplementary Figure 1](#)), mice with prior intestinal infection had a higher sickness score ([Figure 1C](#)). This sickness scoring system included hunched posture, ruffled fur, decreased movement, and altered respiratory rates and quality of breaths ([Figure 1C](#)). Of note, mice with only *ST* intestinal infection showed no weight loss and had reduced sickness scores. When bacterial burden was evaluated at 18 and 33 hours post-*KP* infection, we found significantly higher lung bacterial burden in mice with prior intestinal infection compared with

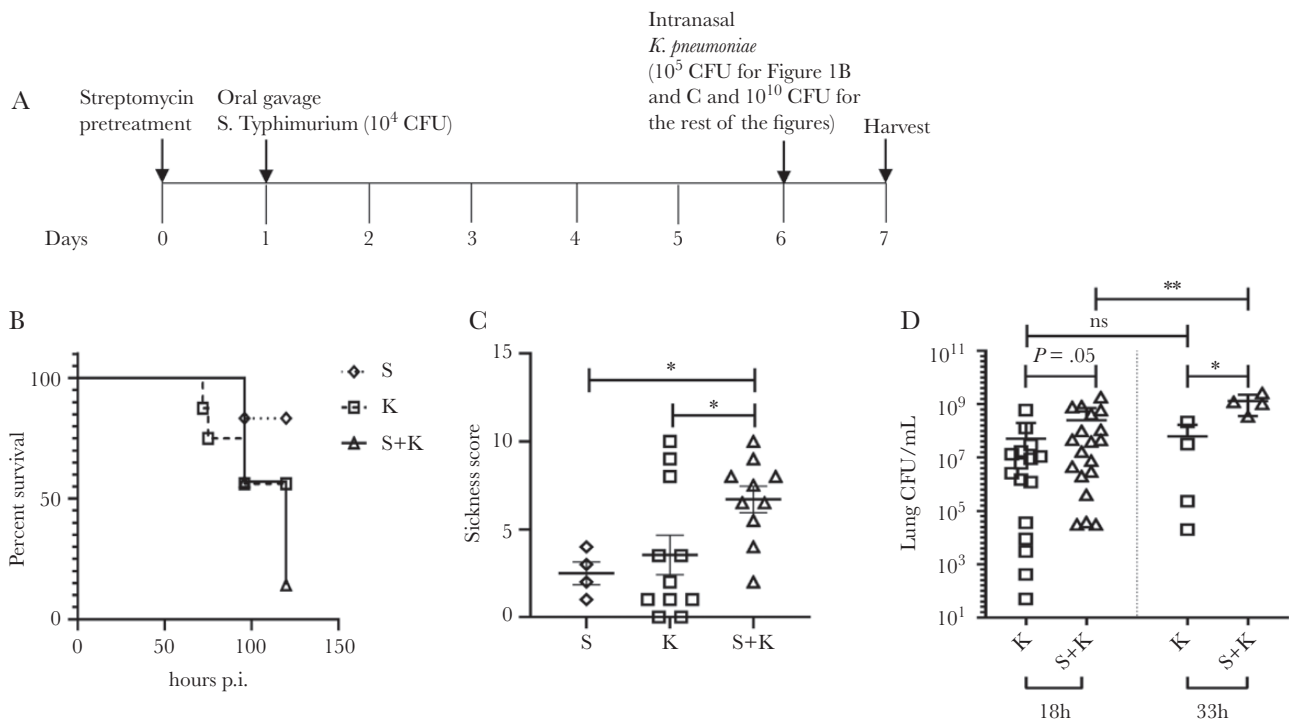


**Figure 1.** Mice with prior *Salmonella enterica* serovar Typhimurium (*S. Typhimurium* [*ST*]) intestinal infection have increased susceptibility to respiratory *Klebsiella pneumoniae* (*KP*) infection. **A**, Time line of this study. **B**, Kaplan-Meier survival curves of mice infected with *ST* intestinal infection (*S*), *KP* infection only (*K*), and mice with prior intestinal *ST* infection and challenged with *KP* infection (*S* + *K*). Statistical analysis was performed using the log-rank (Mantel-Cox) test ( $P = .07$ ) and log-rank test for significant trend ( $P = .02$ ). **C**, Sickness score plots where data represent cumulative results of 2 independent experiments ( $n = 4$ – $6$  for *S*,  $n = 11$  for *K*, and  $n = 10$  for *S* + *K*) and mean  $\pm$  SD.  $*P < .05$ . Statistical analysis was performed using the Kruskal-Wallis test followed by Dunn’s multiple comparison test. **D**, *KP* bacterial load determined in lungs at 18 hours post-*KP* infection in both *K* and *S* + *K* groups. Data represent cumulative results of 3 independent experiments ( $n = 16$  for *K* and  $n = 19$  for *S* + *K*). Lung bacterial loads also determined at 33 hours in both groups ( $n = 4$  for each group,  $n = 1$  experiment). Data represent mean  $\pm$  SD, and statistical significance was determined using the Mann-Whitney test.  $*P < .05$ ;  $**P < .01$ .

mice without prior intestinal infection (Figure 1D). Mice with prior intestinal infection also showed significantly higher lung bacterial burden at 33 hours compared with 18 hours (Figure 1D). We could not isolate any *ST* from lung homogenates of mice with intestinal infection. In addition, in a subset of animals, we performed metagenomic next-generation sequencing (Supplementary Methods) and observed the presence of *ST* in stool samples and *KP* in bronchoalveolar lavage (BAL) fluid (Supplementary Table 1).

#### **Mice With Prior *ST* Intestinal Infection Have Increased Lung Inflammation From Subsequent Respiratory *KP* Infection**

We next examined the degree of lung inflammation by histological analysis of tissue sections from all 4 groups of mice. Histopathological analysis revealed mixed interstitial inflammatory consolidations in mice with *KP* respiratory infection and increased microabscess formation with pyknotic neutrophils in mice co-infected with *ST* and *KP* (Figure 2A; Supplementary Table 2). Uninfected mice and mice with intestinal infection showed normal alveolar and interstitial lung histology (Figure 2A). Upon challenge with *KP* respiratory infection, mice with prior *ST* intestinal infection also showed marked intravascular clustering of polymorphonuclear neutrophils (PMNs), with increased margination, necrotic cluster formation, and extravasation (Figure 2B; Supplementary Figure 2). Intravascular neutrophil clustering was noticeably absent in the other treatment groups. Furthermore, lung sections from mice with intestinal infection and mice with both intestinal and respiratory infection showed scattered microthrombi in capillary-sized vessels, whereas mice with *KP* respiratory infection (with no prior intestinal infection) showed no microthrombus formation (Supplementary Figure 3).

#### **Mice With Prior *ST* Intestinal Infection Have Altered Lung Cytokine Profiles After *KP* Challenge**

The delicate balance between pro- and anti-inflammatory cytokines is crucial in containing pathogens and maintaining tissue repair and homeostasis in the lung [11]. Prior studies have shown the importance of cytokines such as interferon (IFN)- $\gamma$  in recruitment of neutrophils to the lung tissue [15, 16]. We investigated whether intestinal infection affected cytokine production in lung homogenates and whether prior intestinal infection affected this cytokine response to intranasal *KP* challenge. Our results indicate that compared with the uninfected control group, *ST*-infected mice had significantly higher lung levels of IFN- $\gamma$ , monocyte chemoattractant protein-1, and interleukin (IL)-1 $\beta$  (Figure 3 A–C). While Thy1-expressing natural killer (NK) cells [17] and NKp46<sup>+</sup> ILC3 [17] cells are commonly thought to be the sources of IFN- $\gamma$ , there is a mounting evidence that neutrophils are a prominent cellular source of IFN- $\gamma$  during the innate phase of *ST*-induced colitis [18]. It is possible that large numbers of primed neutrophils traffick to the lungs after intestinal

infection, contribute to cytokine production, and increase the potential for neutrophil-mediated pathology or NET formation upon secondary infection [8]. Furthermore, following *KP* challenge, mice with prior intestinal infection had higher levels of IFN- $\gamma$  and lower levels of granulocyte-macrophage colony-stimulating factor (GM-CSF) cytokine production in lung homogenates compared with those without prior intestinal infection (Figure 3A and D). Levels of IL-23, IL-1 $\alpha$ , tumor necrosis factor (TNF)  $\alpha$ , IL-12p70, IL-10, IL-6, IL-27, IL-17A, and IFN- $\beta$  were not significantly different between mice with and without prior intestinal infection (Supplementary Figure 4).

#### **Mice With Prior *ST* Intestinal Infection Have Lower Numbers of Neutrophils in the Lungs After *KP* Challenge**

We next examined the impact of intestinal infection on innate cellular responses in the lung, and also its effect on such responses to *KP* respiratory challenge. We analyzed changes in major innate lung leukocytes (plasmacytoid dendritic cells [pDCs], monocyte-derived dendritic cells [moDCs], CD103<sup>+</sup> DCs, neutrophils, alveolar macrophages [AMs], and interstitial macrophages [IMs]) before and after *KP* challenge in mice infected with *ST* (gating strategy in Supplementary Figure 5A). Consistent with previous studies [19], we observed rapid and robust recruitment of neutrophils to the lungs at 18 hours after *KP* infection compared with uninfected controls. Interestingly, mice with prior intestinal *ST* infection had significantly lower frequencies and total numbers of lung neutrophils following *KP* challenge compared with mice infected with *KP* alone (Figure 4A). Furthermore, the results indicated that frequencies of pDCs increased and moDCs decreased in the lungs of *ST* intestinally infected mice compared with uninfected controls (Figure 4B and C). Following intranasal *KP* challenge, we found a marked increase in frequencies of pDCs and significantly lower frequencies of moDCs in mice with prior *ST* intestinal infection compared with those without prior intestinal infection (Figure 4B and C). No significant differences were observed in frequencies of CD103<sup>+</sup> DCs (Figure 4D) between *KP*-infected mice with and without prior *ST* intestinal infection. Total numbers of pDCs, moDCs, CD103<sup>+</sup> DCs, AMs, and IMs were not different in mice with prior intestinal infection compared with those without prior *ST* intestinal infection (Figure 4; Supplementary Figure 6). We also found higher numbers of neutrophils, pDCs, and IMs and lower numbers of CD103<sup>+</sup> DCs in mice with only *ST* intestinal infection compared with uninfected mice (Figure 4; Supplementary Figure 6).

We also investigated innate-like T cells including MAIT cells, iNKT cells,  $\gamma\delta$  T cells, and natural killer cells as they are known to play an important role in bacterial infections (gating strategy in Supplementary Figure 5B) [7]. No differences were observed in percent frequencies or total number of iNKT cells, MAITs,  $\gamma\delta$  T cells, or NK cells between mice with and without prior intestinal infection (Figure 5). Furthermore, when complete blood counts

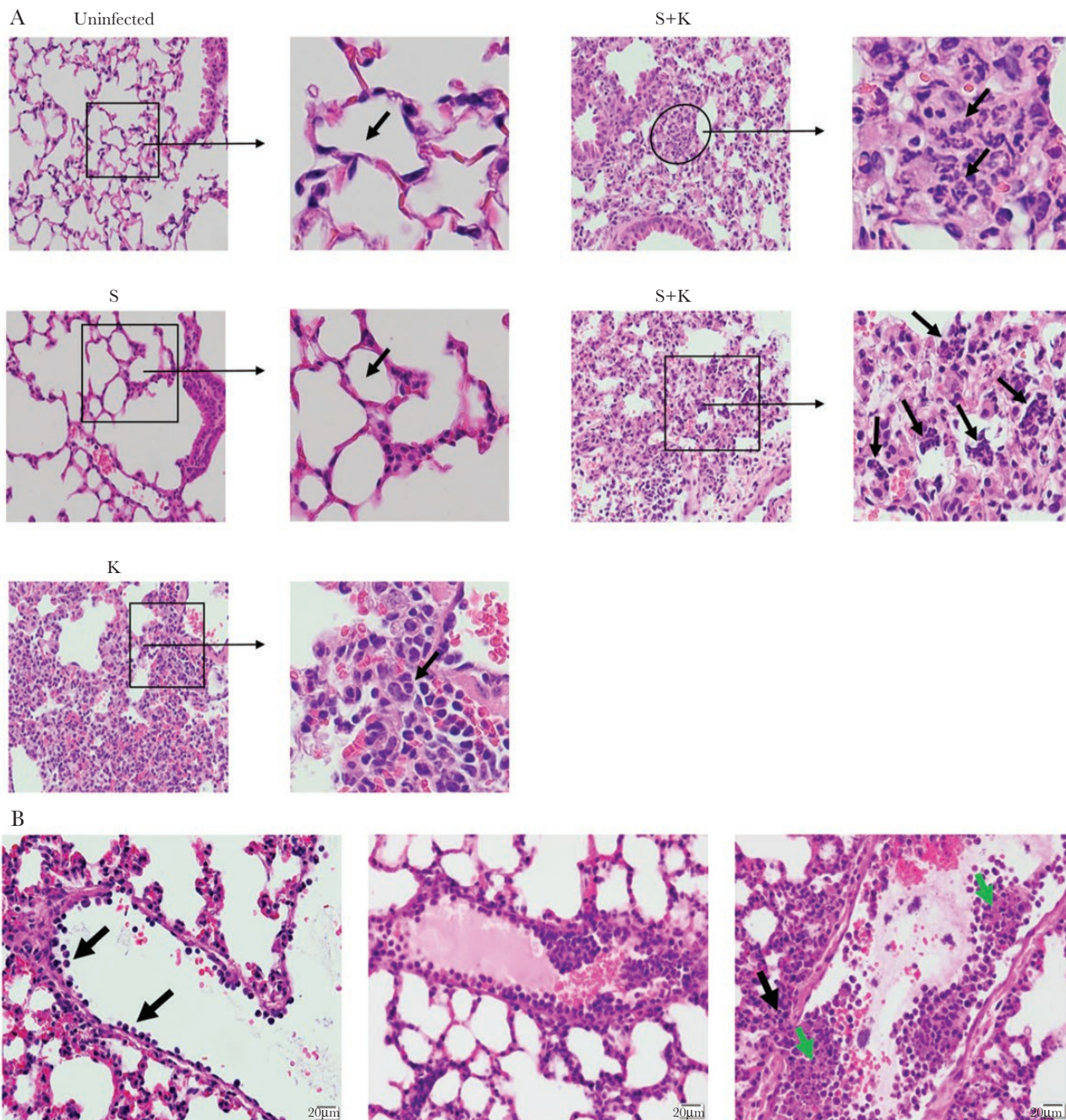


**Figure 2.** Mice with prior *Salmonella enterica* serovar Typhimurium (*S. Typhimurium* [S7]) intestinal infection have increased lung inflammation from subsequent respiratory *Klebsiella pneumoniae* (*KP*) infection, characterized by microabscess, pyknotic neutrophil clusters, and margination, compared with those with no prior intestinal infection. A, Representative images (400× magnification, scale bar = 20 μm) of lung sections stained with hematoxylin and eosin (H&E). Insets show digital magnification of original image. In uninfected mice and in mice with intestinal infection only (S), black arrows show normal lung parenchyma. Mice with respiratory infection only (K) show mixed interstitial inflammatory consolidations, and the black arrow shows a normal neutrophil. In mice with prior intestinal ST infection and challenged with KP infection (S + K), microabscesses are circled and black arrows highlight clusters of pyknotic neutrophils. B, Representative images (H&E, 400× magnification, scale bar = 20 μm) of lung sections of S + K–infected mice. Lung vessels in S + K–infected mice showing neutrophil margination (left, black arrows), margination and clustering (middle), necrotic clusters (right, green arrow), and extravasation (right, black arrow). Data represent cumulative results of 2 independent experiments (n = 2 for UI, n = 10 for S group, n = 9 for K group, and n = 8 for S + K group).

were assessed with a Hemavet analyzer, no significant differences were observed in circulating neutrophils, lymphocytes, monocytes, eosinophils, basophils, or platelets between mice with and without prior intestinal infection (Supplementary Figure 7).

#### Mice With Prior *ST* Intestinal Infection Demonstrate Widespread Lung NETosis After *KP* Challenge

Recent studies have revealed that excessive NET formation plays a role in pathogen-associated lung injury, including in

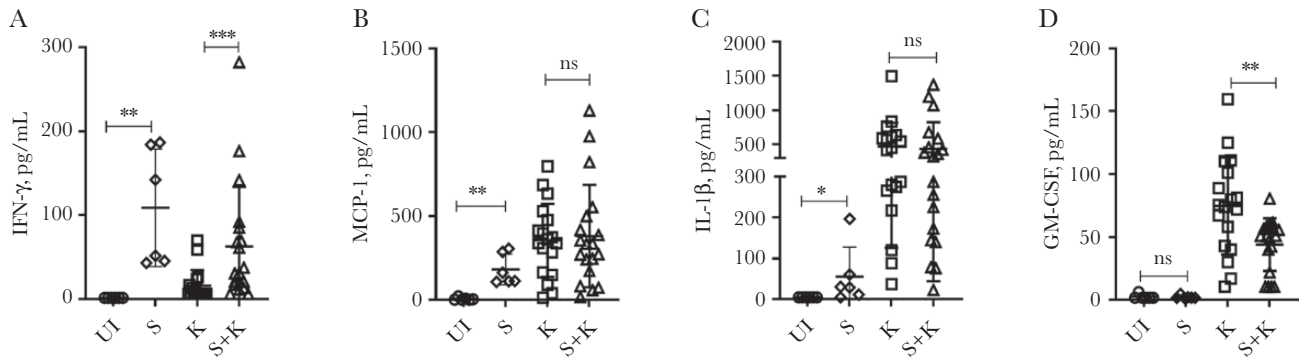


**Figure 3.** Mice with prior *Salmonella enterica* serovar Typhimurium (*S. Typhimurium* [S7]) intestinal infection have altered lung cytokine profiles and altered cytokine responses to respiratory *Klebsiella pneumoniae* (*KP*) infection, compared with those with no prior intestinal infection. Levels of lung inflammatory cytokines (A) interferon- $\gamma$  (minimum detection limit [MDL] = 2.44 pg/mL), (B) monocyte chemoattractant protein-1 (MDL = 2.44 pg/mL), (C) interleukin-1 $\beta$  (MDL = 2.44 pg/mL), and (D) granulocyte-macrophage colony-stimulating factor (MDL = 2.44 pg/mL) were assessed 18 hours post-*KP* challenge via bead-based LEGENDplex mouse inflammation panel 13-plex assay. Data represent 1 experiment for uninfected mice ( $n = 6$ ) and *S7*-infected mice ( $n = 6$ ) and cumulative results of 3 independent experiments for the *K* ( $n = 18$ ) and *S + K* groups ( $n = 19$ ). Error bars represent mean  $\pm$  SD, and significance was determined by Mann-Whitney tests.

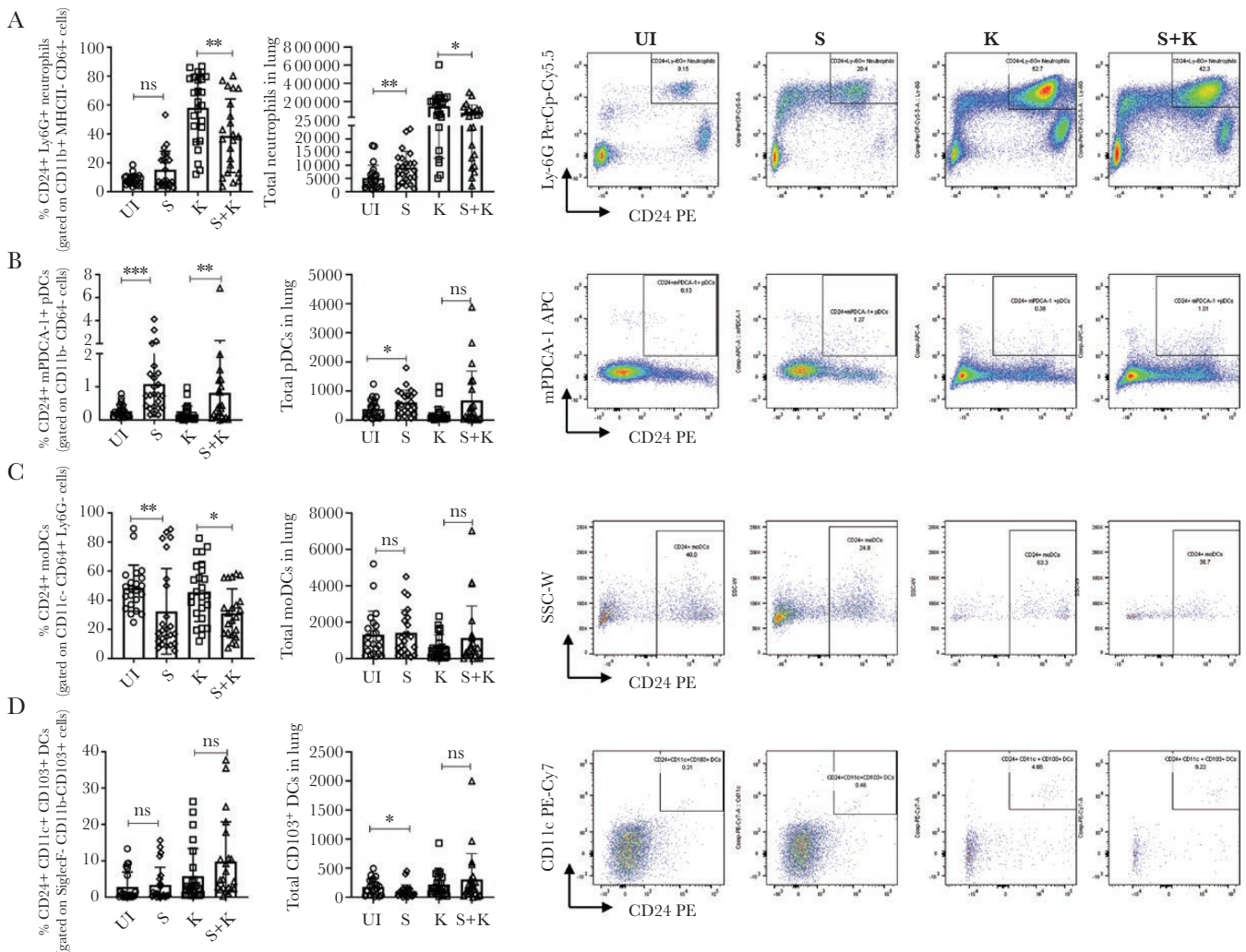


**Figure 4.** Mice with prior *Salmonella enterica* serovar Typhimurium (*S. Typhimurium* [S7]) intestinal infection have altered frequencies of innate cell types in the lung and altered lung innate cellular responses to respiratory *Klebsiella pneumoniae* (*KP*) infection. Percent frequencies, total numbers, and representative fluorescence-activated cell sorting plots of (A) neutrophils, (B) lung plasmacytoid dendritic cells (pDCs), (C) monocytic dendritic cells (moDCs), (D) CD103<sup>+</sup> dendritic cells are shown in uninfected mice (UI), *S7*-infected mice (S), *KP*-infected mice (K), and both *S7* and *KP*-infected mice (S + K). Data represent cumulative results of 5 independent experiments ( $n = 22$  for UI,  $n = 24$  for S,  $n = 25$  for K, and  $n = 22$  for S + K). Error bars represent mean  $\pm$  SD, and statistically significant difference between UI and S or between K and S + K was determined using Mann-Whitney tests.

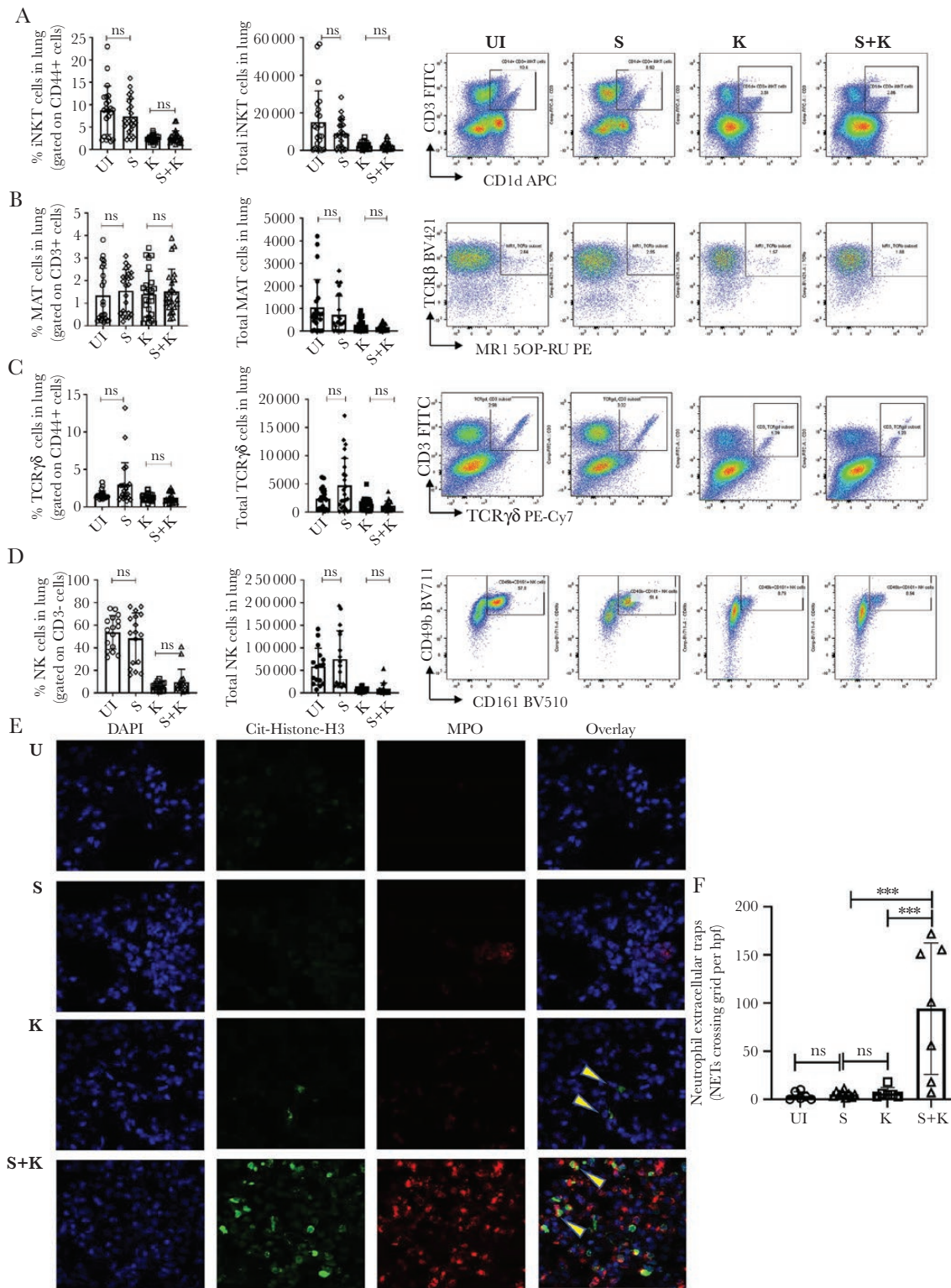


**Figure 5.** Mice with prior *Salmonella enterica* serovar Typhimurium (*S. Typhimurium* [S7]) intestinal infection have no differences in invariant natural killer T (iNKT), mucosal-associated invariant T, T-cell receptor (TCR)  $\gamma\delta$ , or natural killer (NK) cells and have increased neutrophil extracellular trap (NET) formation in lungs from subsequent respiratory *Klebsiella pneumoniae* (*KP*) infection, compared with those with no prior intestinal infection. Percent frequencies, total numbers, and representative fluorescence-activated cell sorting plots of (A) iNKT cells, (B) MAIT cells, (C) TCR  $\gamma\delta$  cells, and (D) NK cells are shown in uninfected mice (UI), *ST*-infected mice (S), *KP*-infected mice (K), and both *ST* and *KP*-infected mice (S + K). Data represent cumulative results of 5 independent experiments ( $n = 22$  for UI,  $n = 24$  for S,  $n = 25$  for K, and  $n = 22$  for S + K). Error bars represent mean  $\pm$  SD, and statistically significant differences between UI and S or between K and S + K were determined using Mann-Whitney tests. E, Using confocal microscopy, NET formation was assessed in all 4 groups, and images were taken at 60 $\times$  magnification. Blue fluorescence = nuclear DNA; green fluorescence = citrullinated histone H3; red fluorescence = myeloperoxidase. NETs are highlighted by yellow arrows in the overlying images. F, Bar graph showing number of NETs crossing grid lines per high power field. One-way analysis of variance with Tukey's post hoc test. \*\*\*  $P < .001$ .

models of bacterial pneumonia [20–23]. Our histopathological analysis revealed clusters of pyknotic neutrophils and thrombus formation in mice with prior intestinal infection (Figure 2; Supplementary Figure 3). It is known that neutrophils constitute a key cellular component of thrombi and participate in thrombosis by releasing NETs [24]. Moreover, we detected higher levels of IFN- $\gamma$  in mice with prior intestinal infection compared with mice without prior intestinal infection (Figure 3), and IFN- $\gamma$  can promote NET formation by neutrophils [25]. We therefore determined whether prior intestinal *ST* infection was associated with increased lung NET formation following intranasal *KP* challenge. We examined citrullinated histones and MPO in the lung tissues of each experimental group by immunofluorescence. We found a significantly higher number of NETs ( $P = .0006$ ) in mice with prior intestinal *ST* infection compared with those without prior intestinal infection (Figure 5 E and F), as demonstrated by the presence of extracellular DNA overlaid with citrullinated histone H3 and MPO (Figure 5E). Mock-infected lungs did not show any staining for citrullinated histone H3 or MPO. We detected minimal to no NETs in lung tissues of mice in the uninfected control group, intestinal *ST* infection alone group, or *KP*-infected alone group, and there was no significant difference between these groups (Figure 5F).

## DISCUSSION

We found that bacterial intestinal infection in mice adversely impacts immunity in the lung, increasing susceptibility to secondary respiratory infection. We show that mice with prior intestinal *ST* infection have higher lung bacterial burden and sickness scores after subsequent *KP* challenge compared with mice without prior *ST* infection. This finding was associated with changes in innate cellular responses, most notably those of neutrophils, which were decreased in the parenchyma, clustering in the lung vasculature, and associated with increased NET formation in those with secondary infection. As neutrophils are essential for pulmonary clearance of bacterial infections such as *KP* [9], it is possible that intestinal infection impairs the recruitment and function of lung neutrophil responses against *KP*, leading to an inability to clear the lung bacterial infection, thereby worsening lung function.

In addition to epidemiological studies showing a higher susceptibility to pulmonary infections after intestinal infection in children [2, 3] and that intestinal diseases are often associated with pulmonary disorders [26], the immunological crosstalk of the lung–gut axis is not well understood. In the context of IBD, it has been proposed that intestinal inflammation and increased cytokine levels create conditions favorable for neutrophil margination onto the lung endothelium [27]. When the lung encounters a secondary insult, neutrophil recruitment, activation, and extravasation could mediate lung tissue injury and IBD-induced respiratory diseases [8, 28]. Our knowledge of

how intestinal infection impacts the recruitment, extravasation, and function of neutrophils in tissues outside of the intestine is limited. Studies have shown that GM-CSF plays an important role in neutrophil accumulation [29, 30], and GM-CSF has been shown to be protective in preclinical models of pneumonia-associated lung injury [31]. We found a significantly lower lung GM-CSF response to *KP* infection in mice with prior intestinal infection, which may decrease the lung's ability to recruit circulating neutrophils, resulting in an increased susceptibility to infection. In line with this, we also detected increased NET formation and microthrombosis in *KP* infection in mice with prior intestinal *ST* infection as compared with mice without prior intestinal infection. It is likely that NETs and NET-associated factors, including histones and granule proteases, mediate vascular and tissue injury and contribute to microthrombosis [14, 32–34]. The activation of NETosis, the regulated cell death process leading to NET formation, also causes changes in neutrophil morphology including cell membrane rupture and neutrophil death [35]. We speculate that prior intestinal infection induces NET formation, contributing to lower numbers of viable neutrophils in the lungs. Further studies examining the mechanisms governing neutrophil activation and NET formation in the lungs after intestinal infection are warranted.

Nonconventional T lymphocytes including MAIT cells, *i*NKT cells, and  $\gamma\delta$ -T cells have tissue-homing properties and have been implicated in protection against respiratory bacterial infections [7]. Here, we found no differences in the frequencies or number of these cells between the groups tested. Likewise, except for IFN- $\gamma$  we did not find any differences in cytokines that have been implicated in lung defense against bacterial pathogens, including IL-17A [36], TNF- $\alpha$  [37], and IL-10 [38]. Both protective [39] and detrimental [40] roles of IFN- $\gamma$  have been reported in bacterial infections, and we found significant increases in lung IFN- $\gamma$  production in mice with intestinal infection. Numerous studies have shown that IFN- $\gamma$  produced by activated CD4<sup>+</sup> and CD8<sup>+</sup> T cells and NK cells plays an important role in protective immunity to *Salmonella* [41, 42]. Although we did not observe differences in NK cell numbers in mice with and without prior intestinal infection, it is possible that activated T cells responding to conserved microbial epitopes are recruited early to the lung after intestinal infection and are a major source of IFN- $\gamma$  production. However, the importance of T-cell activation and IFN- $\gamma$  production in our co-infection model is unclear and merits further investigation. Modulation of respiratory DCs during *KP* infection has been reported before by Hackstein et al. [43]. Although we did not observe differences in total number of DCs, we observed higher frequencies of pDCs in the lungs of mice with prior intestinal infection, and this may be related to the role of respiratory pDCs in tissue repair [44]. Alternatively, accumulation of pDCs in lungs post-intestinal infection may be involved in the initiation of inflammation



and antigen-specific T-cell responses [45]. Moreover, frequencies of moDCs, which may contribute to control of secondary respiratory *KP* infection, were decreased in mice with prior intestinal infection [46]. Further studies are necessary to address the functional role of pDCs and moDCs during bacterial pneumonia after intestinal infection.

Our study has several limitations. First, we did not account for the effect of the preexisting intestinal microbiota; however, all mice were purchased from the same source and were cohoused before infection. Second, we did not evaluate serum levels of IL-6, TNF- $\alpha$ , IFN- $\gamma$ , and vascular endothelial growth factor [27], or neutrophil chemokines such as keratinocyte-derived chemokine (KC), macrophage inflammatory protein 2, CXC receptor 2, and CXC ligand 5 [47], which would further our understanding of lung neutrophil trafficking following intestinal inflammation. Third, we have not investigated the role of innate lymphoid cells, which have been shown to be recruited from the gut to the lungs in response to inflammation [48]. Fourth, we have not tested the impact of lower/graded doses of *KP* challenge in mice with prior intestinal infection. Lastly, we emphasize that our study lacks experiments aimed at determining the mechanisms leading to increased lung pathology following intestinal infection. We hypothesize that in secondary infections neutrophil response and NET production require a fine balance: Underactivity can lead to risk for increased pathogen replication and invasion, whereas overactivity can result in excessive inflammation and tissue damage. Future experiments examining the effect of neutrophil depletion and the effect of NET inhibitors and NET-dismantling agents such as DNase are warranted.

In conclusion, the present study demonstrates that infection in the gut adversely impacts immunity in the lung. This report opens up potential avenues for investigating the immunological crosstalk between the lung and gut during enteric infection. While epidemiological studies have demonstrated this lung-gut association, we provide here novel findings that intestinal infection modulates neutrophil and cytokine responses in the lung, resulting in an increased susceptibility to a secondary pneumonia challenge. These data have the potential to inform efforts to prevent and treat respiratory infections in those with intestinal infection or inflammation.

### Supplementary Data

Supplementary materials are available at Open Forum Infectious Diseases online. Consisting of data provided by the authors to benefit the reader, the posted materials are not copyedited and are the sole responsibility of the authors, so questions or comments should be addressed to the corresponding author.

### Acknowledgments

We would like to thank Cole Anderson, Michael Graves, Alexandra Heitkamp, and Melanie Prettyman for their technical assistance.

**Financial support.** This work was supported in part by grant W81XWH-17-1-0109 from the Department of Defense (to D.T.L.)

and by the National Institutes of Health (R01HD093826 to C.C.Y. and R01AI130378 to D.T.L.). This work was supported by the University of Utah Flow Cytometry Facility, in addition to the National Cancer Institute through Award Number 5P30CA042014-24, and CMC animal facility.

**Potential conflicts of interest.** C.C.Y. authored a US patent (patent no. 10,232,023 B2) held by the University of Utah for the use of NET-inhibitory peptides for the “treatment of and prophylaxis against inflammatory disorders,” for which PEEL Therapeutics, Inc., holds the exclusive license. All authors have submitted the ICMJE Form for Disclosure of Potential Conflicts of Interest. Conflicts that the editors consider relevant to the content of the manuscript have been disclosed.

**Author contributions.** S.T. and D.T.L. designed and directed the project. S.T., O.J., and M.J.C. carried out the experiments. D.T.L., A.H.G., K.J.W., and C.C.Y. contributed to data analysis. S.T. and D.T.L. wrote the paper. P.H.S. and C.L. conducted metagenomic next-generation sequencing. T.W. analyzed metagenomic sequencing data. All authors discussed the results and commented on the manuscript.

**Patient consent.** The study does not include factors necessitating patient consent.

### References

1. Liu L, Oza S, Hogan D, et al. Global, regional, and national causes of under-5 mortality in 2000-15: an updated systematic analysis with implications for the Sustainable Development Goals. *Lancet* **2016**; 388:3027-35.
2. Leung DT, Das SK, Malek MA, et al. Concurrent pneumonia in children under 5 years of age presenting to a diarrheal hospital in Dhaka, Bangladesh. *Am J Trop Med Hyg* **2015**; 93:831-5.
3. Schmidt WP, Cairncross S, Barreto ML, et al. Recent diarrhoeal illness and risk of lower respiratory infections in children under the age of 5 years. *Int J Epidemiol* **2009**; 38:766-72.
4. Tulic MK, Piche T, Verhasselt V. Lung-gut cross-talk: evidence, mechanisms and implications for the mucosal inflammatory diseases. *Clin Exp Allergy* **2016**; 46:519-28.
5. Schuijt TJ, Lankelma JM, Scicluna BP, et al. The gut microbiota plays a protective role in the host defence against pneumococcal pneumonia. *Gut* **2016**; 65:575-83.
6. Budden KE, Gellatly SL, Wood DLA, et al. Emerging pathogenic links between microbiota and the gut-lung axis. *Nat Rev Microbiol* **2017**; 15:55-63.
7. Ivanov S, Paget C, Trottein F. Role of non-conventional T lymphocytes in respiratory infections: the case of the pneumococcus. *PLoS Pathog* **2014**; 10:e1004300.
8. Mateer SW, Maltby S, Marks E, et al. Potential mechanisms regulating pulmonary pathology in inflammatory bowel disease. *J Leukoc Biol* **2015**; 98:727-37.
9. Xiong H, Carter RA, Leiner IM, et al. Distinct contributions of neutrophils and CCR2+ monocytes to pulmonary clearance of different *Klebsiella pneumoniae* strains. *Infect Immun* **2015**; 83:3418-27.
10. Barthel M, Hapfelmeier S, Quintanilla-Martínez L, et al. Pretreatment of mice with streptomycin provides a *Salmonella enterica* serovar Typhimurium colitis model that allows analysis of both pathogen and host. *Infect Immun* **2003**; 71:2839-58.
11. Altmeyer M, Barthel M, Eberhard M, et al. Absence of poly(ADP-ribose) polymerase 1 delays the onset of *Salmonella enterica* serovar Typhimurium-induced gut inflammation. *Infect Immun* **2010**; 78:3420-31.
12. Kaiser P, Hardt WD. *Salmonella typhimurium* diarrhea: switching the mucosal epithelium from homeostasis to defense. *Curr Opin Immunol* **2011**; 23:456-63.
13. Burkholder T, Foltz C, Karlsson E, et al. Health evaluation of experimental laboratory mice. *Curr Protoc Mouse Biol* **2012**; 2:145-65.
14. Yost CC, Schwertz H, Cody MJ, et al. Neonatal NET-inhibitory factor and related peptides inhibit neutrophil extracellular trap formation. *J Clin Invest* **2016**; 126:3783-98.
15. Yamada M, Gomez JC, Chugh PE, et al. Interferon- $\gamma$  production by neutrophils during bacterial pneumonia in mice. *Am J Respir Crit Care Med* **2011**; 183:1391-401.
16. Pechous RD. With friends like these: the complex role of neutrophils in the progression of severe pneumonia. *Front Cell Infect Microbiol* **2017**; 7:160.
17. Kupz A, Scott TA, Belz GT, et al. Contribution of Thyl+ NK cells to protective IFN- $\gamma$  production during *Salmonella typhimurium* infections. *Proc Natl Acad Sci U S A* **2013**; 110:2252-7.
18. Spees AM, Kingsbury DD, Wangdi T, et al. Neutrophils are a source of gamma interferon during acute *Salmonella enterica* serovar Typhimurium colitis. *Infect Immun* **2014**; 82:1692-7.
19. Zhang S, Kingsley RA, Santos RL, et al. Molecular pathogenesis of *Salmonella enterica* serotype Typhimurium-induced diarrhea. *Infect Immun* **2003**; 71:1-12.

20. Narasaraju T, Yang E, Samy RP, et al. Excessive neutrophils and neutrophil extracellular traps contribute to acute lung injury of influenza pneumonitis. *Am J Pathol* **2011**; 179:199–210.
21. Porto BN, Stein RT. Neutrophil extracellular traps in pulmonary diseases: too much of a good thing? *Front Immunol* **2016**; 7:311.
22. Lefrançois E, Mallavia B, Zhuo H, Calfee CS, Looney MR. Maladaptive role of neutrophil extracellular traps in pathogen-induced lung injury. *JCI Insight* **2018**; 3:e98178.
23. Pulavendran S, Prasanthi M, Ramachandran A, et al. Production of neutrophil extracellular traps contributes to the pathogenesis of *Francisella* tularemia. *Frontiers Immunol* **2020**; 11.
24. von Brühl ML, Stark K, Steinhart A, et al. Monocytes, neutrophils, and platelets cooperate to initiate and propagate venous thrombosis in mice in vivo. *J Exp Med* **2012**; 209:819–35.
25. Bertin FR, Rys RN, Mathieu C, et al. Natural killer cells induce neutrophil extracellular trap formation in venous thrombosis. *J Thromb Haemost* **2019**; 17:403–14.
26. Kelly MG, Frizelle FA, Thornley PT, et al. Inflammatory bowel disease and the lung: is there a link between surgery and bronchiectasis? *Int J Colorectal Dis* **2006**; 21:754–7.
27. Scaldaferrri F, Vetrano S, Sans M, et al. VEGF-A links angiogenesis and inflammation in inflammatory bowel disease pathogenesis. **2009**; 136:585–95.e5.
28. Margraf A, Ley K, Zarbock A. Neutrophil recruitment: from model systems to tissue-specific patterns. *Trends Immunol* **2019**; 40:613–34.
29. Khajah M, Millen B, Cara DC, et al. Granulocyte-macrophage colony-stimulating factor (GM-CSF): a chemoattractive agent for murine leukocytes in vivo. *J Leukoc Biol* **2011**; 89:945–53.
30. Laan M, Prause O, Miyamoto M, et al. A role of GM-CSF in the accumulation of neutrophils in the airways caused by IL-17 and TNF-alpha. *Eur Respir J* **2003**; 21:387–93.
31. Quinton LJ. GM-CSF: a double dose of protection during pneumonia. *Am J Physiol Lung Cell Mol Physiol* **2012**; 302:L445–6.
32. Cheng OZ, Palaniyar N. NET balancing: a problem in inflammatory lung diseases. *Front Immunol* **2013**; 4:1.
33. Martinod K, Wagner DD. Thrombosis: tangled up in NETs. *Blood* **2014**; 123:2768–76.
34. Fuchs TA, Brill A, Wagner DD. Neutrophil extracellular trap (NET) impact on deep vein thrombosis. *Arterioscler Thromb Vasc Biol* **2012**; 32:1777–83.
35. Brinkmann V, Zychlinsky A. Beneficial suicide: why neutrophils die to make NETs. *Nat Rev Microbiol* **2007**; 5:577–82.
36. Simonian PL, Roark CL, Wehrmann F, et al. IL-17A-expressing T cells are essential for bacterial clearance in a murine model of hypersensitivity pneumonitis. *J Immunol* **2009**; 182:6540–9.
37. Skerrett SJ, Martin TR, Chi EY, et al. Role of the type 1 TNF receptor in lung inflammation after inhalation of endotoxin or *Pseudomonas aeruginosa*. *Am J Physiol* **1999**; 276:L715–27.
38. Kang MJ, Jang AR, Park JY, et al. IL-10 protects mice from the lung infection of *Acinetobacter baumannii* and contributes to bacterial clearance by regulating STAT3-mediated MARCO expression in macrophages. *Front Immunol* **2020**; 11:270.
39. Moore TA, Perry ML, Getsoian AG, et al. Divergent role of gamma interferon in a murine model of pulmonary versus systemic *Klebsiella pneumoniae* infection. *Infect Immun* **2002**; 70:6310–8.
40. Schultz MJ, Rijnveld AW, Speelman P, et al. Endogenous interferon-gamma impairs bacterial clearance from lungs during *Pseudomonas aeruginosa* pneumonia. *Eur Cytokine Netw* **2001**; 12:39–44.
41. Mitrücker H-W, Köhler A, Kaufmann SHE. Characterization of the murine T-lymphocyte response to *Salmonella enterica* serovar Typhimurium infection. *Infect Immun* **2002**; 70:199–203.
42. Ravindran R, McSorley SJ. Tracking the dynamics of T-cell activation in response to *Salmonella* infection. *Immunology* **2005**; 114:450–8.
43. Hackstein H, Kranz S, Lippitsch A, et al. Modulation of respiratory dendritic cells during *Klebsiella pneumoniae* infection. *Respir Res* **2013**; 14:91.
44. Gregorio J, Meller S, Conrad C, et al. Plasmacytoid dendritic cells sense skin injury and promote wound healing through type I interferons. *J Exp Med* **2010**; 207:2921–30.
45. Takagi H, Fukaya T, Eizumi K, et al. Plasmacytoid dendritic cells are crucial for the initiation of inflammation and T cell immunity in vivo. *Immunity* **2011**; 35:958–71.
46. Bieber K, Autenrieth SE. Dendritic cell development in infection. *Mol Immunol* **2020**; 121:111–7.
47. Tateda K, Moore TA, Newstead MW, et al. Chemokine-dependent neutrophil recruitment in a murine model of *Legionella* pneumonia: potential role of neutrophils as immunoregulatory cells. *Infect Immun* **2001**; 69:2017–24.
48. Mjösberg J, Rao A. Lung inflammation originating in the gut. *Science* **2018**; 359:36–7.